foundations

MDPI

Article

Binding and Recombination Energies of Quasi-One-Dimensional Excitonic Complexes in Ellipsoidal Quantum Dot

David B. Hayrapetyan

General Physics and Quantum Nanostructures, Russian-Armenian University, 123 Hovsep Emin Str., Yerevan 0051, Armenia; david.hayrapetyan@rau.am; Tel.: +374-93934311

Abstract: In the framework of the effective mass approximation, negative and positive trions, exciton, and biexciton states are investigated in strongly prolate ellipsoidal quantum dots by the variational method. Since the ellipsoidal quantum dot has a prolate character, all excitonic complexes are considered quasi-one-dimensional. As in such a system, the analytical solution does not exist for the many-particle problem, it is solved by the variational method. The trial variation functions based on the one-particle wave functions are used to construct the wavefunctions for the excitonic complexes. The energy spectrum, binding, and recombination energies dependent on the geometrical parameters of the ellipsoidal quantum dots are calculated for the excitons, negative and positive trions, and biexcitons. The radiative lifetime of exciton complexes in ellipsoid is estimated.

Keywords: biexciton; trion; ellipsoidal quantum dot; binding energy; recombination energy; lifetime

Citation: Hayrapetyan, D.B. Binding and Recombination Energies of Quasi-One-Dimensional Excitonic Complexes in Ellipsoidal Quantum Dot. *Foundations* **2022**, *2*, 219–227. https://doi.org/10.3390/foundations2010015

Academic Editors: Cristina Achim, Ana Bratu and Mioara Petrus

Received: 13 January 2022
Accepted: 7 February 2022
Published: 12 February 2022

1. Introduction

In quantum dots (QD), optically generated excitonic complexes can exist in different states: neutral monoexciton X (one electron and one hole $e-h$), negatively charged exciton X^- ($2e-h$), positively charged exciton X^+ ($e-2h$), biexciton XX ($2e-2h$), etc.

Investigation of the excitonic complexes of semiconductor QDs, where the parameters can be tuned in a wide range, are of importance both from the point of view of fundamental and applied physics. The investigation of excitonic complexes in bulk semiconductors is difficult to achieve experimentally; the reason for this is the small value of the binding energy [1–5]. However, this problem does not arise in the semiconductor nanostructures, particularly in QDs because of the effects of size quantization [6–10]. Thus, biexciton and trion states in quantum nanostructures with different shapes and geometries need to be theoretically and experimentally investigated. The realization of these complexes in QDs can be applied for the development of quantum information processes. Such structures can act as quantum bits, which are the fundamental building blocks of quantum computation [11,12]. As it is known, the progress of semiconductor nanotechnologies made it possible to develop QDs with various shapes and dimensions [13–19]. Thus, the theoretical and experimental investigation of these structures is an actual problem, due to the application of these structures in many areas of novel technologies.

The exciton and biexciton are neutral compound quasiparticles, which are bosons. This means they have integer spin, thus spin-orbit coupling can be neglected. Trions are positively or negatively charged quasiparticles, which are fermions. The negative and positive trions are also called negative and positive biexcitonic ions, respectively, whose existence was suggested by Lampert [20]. Since biexcitons are also integer-spin bosons, they are expected to obey the same Bose statistics as excitons, including Bose narrowing of the energy distribution [21–24].

In this work, the exciton, trion, and biexciton states are investigated in a strong prolate ellipsoidal quantum dot (SPEQD) with the help of the variational method. The advantage of the ellipsoidal QD compared to the spherical QD is that it has two geometrical

parameters. This mentioned peculiarity allows control of the energy spectra [25–29]. The prolate character of the ellipsoidal QD means that the excitonic complexes inside the SPEQD will be one-dimensional. The novelty of the current work is connected with the consideration of the quasi-one-dimensional excitonic complexes in semiconductor QD with prolate character. This specific character of the QD adds to the disposition of the particles along the one direction. Thus, the physical properties of the system will have the same behavior as the one-dimensional systems.

2. Materials and Methods

The quasi-one-dimensional excitonic complexes will be considered in SPEQD with impenetrable walls. Then, the potential energy of the particles in cylindrical coordinates have the following form:

$$\hat{U}(\rho,\varphi,z)=\begin{cases} 0, & \frac{\rho^2}{a^2}+\frac{z^2}{c^2}\leq 1 \\ \infty, & \frac{\rho^2}{a^2}+\frac{z^2}{c^2}>1 \end{cases}, \; a \ll c \tag{1}$$

where a and c, are the small and large semiaxes of the SPEQD, respectively. All dimensionless lengths and energies in the problem are measured in the effective Bohr radius of the electron $a_e=\hbar^2\varepsilon/m_e^*e^2$, the effective Rydberg energy $E_R=\hbar^2/2m_e^*a_e^2$ of the electron, m_e^* is the effective mass of the electron, ε is the dielectric constant, and e is the elementary charge.

Because of the prolate geometry of the SPEQD, the radial direction size quantization will be much more than in the axial direction. Therefore, the exciton, trions, and biexciton can be considered as quasi-one-dimensional. A detailed description of the one-dimensional character of exciton complexes in SPEQD can be found in [18]. Strong size quantization in the radial direction is so strong that one can neglect the interparticle interaction in this direction. In this approximation, the Hamiltonian of the exciton (X), negative trion (X^-), positive trion (X^+), and biexciton (XX) has the form:

$$\begin{aligned}
&\hat{H}_X\left(\vec{r}_1,\vec{r}_a\right)=\sum_j\frac{\hat{P}_j^2}{2m_j^*}+\hat{V}_{\text{int}}(z_1,z_a)+\sum_j\hat{U}_{conf}\left(\vec{r}_j\right),\; j=\{1,a\}\\
&\hat{H}_{X^-}\left(\vec{r}_1,\vec{r}_2,\vec{r}_a\right)=\sum_j\frac{\hat{P}_j^2}{2m_j^*}+\hat{V}_{\text{int}}(z_1,z_2,z_a)+\sum_j\hat{U}_{conf}\left(\vec{r}_j\right),\; j=\{1,2,a\}\\
&\hat{H}_{X^+}\left(\vec{r}_1,\vec{r}_a,\vec{r}_b\right)=\sum_j\frac{\hat{P}_j^2}{2m_j^*}+\hat{V}_{\text{int}}(z_1,z_a,z_b)+\sum_j\hat{U}_{conf}\left(\vec{r}_j\right),\; j=\{1,a,b\}\\
&\hat{H}_{XX}\left(\vec{r}_1,\vec{r}_2,\vec{r}_a,\vec{r}_b\right)=\sum_j\frac{\hat{P}_j^2}{2m_j^*}+\hat{V}_{\text{int}}(z_1,z_2,z_a,z_b)+\sum_j\hat{U}_{conf}\left(\vec{r}_j\right),\; j=\{1,2,a,b\}
\end{aligned} \tag{2}$$

where $\vec{r}_1$ and $\vec{r}_2$ are coordinates of electrons, and $\vec{r}_a$ and $\vec{r}_b$ are coordinates of holes. The confinement potential has the form (1) for all types of particles. Here, $\hat{V}_{\text{int}}$ is the one-dimensional interparticle interaction energy and has the following form:

$$\begin{aligned}
&V_{\text{int}}(z_1,z_a)=-\frac{e^2}{\varepsilon|z_1-z_a|},\\
&V_{\text{int}}(z_1,z_2,z_a)=\frac{e^2}{\varepsilon|z_1-z_2|}-\frac{e^2}{\varepsilon|z_1-z_a|}-\frac{e^2}{\varepsilon|z_2-z_a|},\\
&V_{\text{int}}(z_1,z_a,z_b)=\frac{e^2}{\varepsilon|z_a-z_b|}-\frac{e^2}{\varepsilon|z_1-z_a|}-\frac{e^2}{\varepsilon|z_2-z_b|},\\
&V_{\text{int}}(z_1,z_2,z_a,z_b)=\frac{e^2}{\varepsilon|z_1-z_2|}+\frac{e^2}{\varepsilon|z_a-z_b|}-\frac{e^2}{\varepsilon|z_1-z_a|}-\frac{e^2}{\varepsilon|z_1-z_b|}-\frac{e^2}{\varepsilon|z_2-z_a|}-\frac{e^2}{\varepsilon|z_2-z_b|}.
\end{aligned} \tag{3}$$

Each particle of the excitonic complexes moves in a two-dimensional infinitely deep well in the radial direction. According to the adiabatic approximation, the wave function of the system is sought in the form:

$$\begin{aligned}
&\Phi_X\left(\vec{r}_1,\vec{r}_a\right)=\Psi_X(z_1,z_a)\chi_X\left(\vec{\rho}_1(z_1),\vec{\rho}_a(z_a)\right),\\
&\Phi_{X^-}\left(\vec{r}_1,\vec{r}_2,\vec{r}_a\right)=\Psi_{X^-}(z_1,z_2,z_a)\chi_{X^-}\left(\vec{\rho}_1(z_1),\vec{\rho}_2(z_2),\vec{\rho}_a(z_a)\right)\\
&\Phi_{X^+}\left(\vec{r}_1,\vec{r}_a,\vec{r}_b\right)=\Psi_{X^+}(z_1,z_a,z_b)\chi_{X^+}\left(\vec{\rho}_1(z_1),\vec{\rho}_a(z_a),\vec{\rho}_b(z_b)\right)\\
&\Phi_{XX}\left(\vec{r}_1,\vec{r}_2,\vec{r}_a,\vec{r}_b\right)=\Psi_{XX}(z_1,z_2,z_a,z_b)\chi_{XX}\left(\vec{\rho}_1(z_1),\vec{\rho}_2(z_2),\vec{\rho}_a(z_a),\vec{\rho}_b(z_b)\right),
\end{aligned} \tag{4}$$

where Ψ are wave functions of the slow subsystem in the axial direction, and χ are wave functions of the fast subsystem in the radial direction. The variables of the slow subsystem play the role of constant parameters in the wave function of the fast subsystem [25]. At a fixed value of the coordinate z, the motion of each particle is localized in a two-dimensional potential well with the effective width:

$$\mathrm{L}(z_j)=a\sqrt{1-\frac{{z_j}^2}{c^2}} \tag{5}$$

One-particle wave functions and energies in a SPEQD from Ref. [30] are used for the variational calculations of the one-dimensional exciton, trions, and biexciton states in SPEQD. In the mentioned article, the adiabatic approximation is used for the strong size quantization regime and the results are in good agreement with the results of numerical methods. In this approximation, the eigenfunctions and eigenvalues for a particle in the SPEQD are presented in the following form:

$$\psi_{n,m,N}(\rho,\varphi,z)=\frac{e^{im\varphi}}{\sqrt{2\pi}}\frac{\sqrt{2}J_m(\alpha_{n,m}\rho/L(z))}{L(z)J_{m+1}(\alpha_{n,m})}\sqrt[4]{\frac{\alpha_{n,m}}{ac}}\frac{1}{2^{\frac{N}{2}}\sqrt[4]{\pi}(N!)^{\frac{1}{2}}}e^{-\frac{\alpha_{n,m}}{2ac}z^2}H_N\left(\sqrt{\frac{\alpha_{n,m}}{ac}}z\right), \tag{6}$$

$$E=\frac{\alpha_{n,m}^2}{a^2}+\frac{2\alpha_{n,m}}{ac}\left(N+\frac{1}{2}\right). \tag{7}$$

Here, $m=0,\pm1,\pm2,\ldots$ is the magnetic quantum number, $n=1,2,3,\ldots$ is the radial quantum number, $N=0,1,2,\ldots$ is oscillator quantum number, $H_N(z)$ are Hermite polynomials, $J_m(\rho)$, and $\alpha_{n+1,m}$ are Bessel functions of the first kind and their zeros, correspondingly.

The calculation of the exciton and biexciton ground state energies as dependent on the geometric parameters of the SPEQD will be performed using the variational method. The variational function for the excitonic complexes will be constructed using the single-particle wave functions and can be presented in the following form [31–33]:

$$\begin{aligned}
&\Psi_X^{trial}(z_1,z_a)=C_X\psi_{100}(z_1)\psi_{100}(z_a)e^{-\lambda z_{1a}},\\
&\Psi_{X^-}^{trial}(z_1,z_2,z_a)=C_{X^-}\psi_{100}(z_1)\psi_{100}(z_2)\psi_{100}(z_a)\\
&\qquad\times\sum_{i_1i_2i_{12}}\sum_{j_1j_2j_{12}}c_{i_1i_2i_{12}j_1j_2j_{12}}(1+P_{12})e^{-\alpha_{i_1}^{1a}\rho_{1a}^2-\alpha_{i_2}^{2a}\rho_{2a}^2-\alpha_{i_{12}}^{12}\rho_{12}^2}\times e^{-\beta_{j_1}^{1a}z_{1a}^2-\beta_{j_2}^{2a}z_{2a}^2-\beta_{j_{12}}^{12}z_{12}^2},\\
&\Psi_{X^+}^{trial}(z_1,z_a,z_b)=C_{X^+}\psi_{100}(z_1)\psi_{100}(z_2)\psi_{100}(z_a)\\
&\qquad\times\sum_{i_ai_bi_{ab}}\sum_{j_aj_bj_{ab}}c_{i_ai_bi_{ab}j_aj_bj_{ab}}(1+P_{ab})e^{-\alpha_{ia}^{1a}\rho_{1a}^2-\alpha_{ib}^{1b}\rho_{1b}^2-\alpha_{iab}^{ab}\rho_{ab}^2}\times e^{-\beta_{ja}^{1a}z_{1a}^2-\beta_{jb}^{1b}z_{1b}^2-\beta_{jab}^{ab}z_{ab}^2},\\
&\Psi_{XX}^{trial}(z_1,z_2,z_a,z_b)=C_{XX}\psi_{100}(z_1)\psi_{100}(z_2)\psi_{100}(z_a)\psi_{100}(z_b)\\
&\qquad\times e^{-\gamma z_{ab}}e^{-\alpha(z_{1a}+z_{2b})-\beta(z_{1b}+z_{2a})}e^{-\alpha(z_{1b}+z_{2a})-\beta(z_{1a}+z_{2b})}
\end{aligned} \tag{8}$$

where C are normalization constants, $z_{jk}=\left|z_j-z_k\right|$, $j,k=\{1,2,a,b\}$, $P_{12}(P_{ab})$ is the permutation operator interchanging the electron (hole) indices $1\leftrightarrow2$ ($a\leftrightarrow b$), α, β, γ, λ, $c_{i_1i_2i_{12}j_1j_2j_{12}}$, $\alpha_{i_{jk}}^{jk}$ and $\beta_{i_{jk}}^{jk}$ $j,k=\{1,2,a,b\}$ are variational parameters, which describe the

relative position of the electron and hole in the radial plane and axial direction, respectively. In Equation (7), summations start from 1 and run to M_{jk} over indices i_{1a} and i_{2a}, to N_{jk} over j_{1a} and j_{2a}, and to M_{12} and N_{12} over i_{12} and j_{12}. For the calculations, $M_{jk} = N_{jk} = 2$ and $M_{12} = N_{12} = 3$ were used [33]. All variational parameters are determined after minimizing the integrals:

$$\begin{aligned} E_X &= \left\langle \Psi_X^{trial}(\vec{r}_1, \vec{r}_a) \middle| \hat{H}_X \middle| \Psi_X^{trial}(\vec{r}_1, \vec{r}_a) \right\rangle, \\ E_{X^-} &= \left\langle \Psi_{X^-}^{trial}(\vec{r}_1, \vec{r}_2, \vec{r}_a) \middle| \hat{H}_{X^-} \middle| \Psi_{X^-}^{trial}(\vec{r}_1, \vec{r}_2, \vec{r}_a) \right\rangle, \\ E_{X^+} &= \left\langle \Psi_{X^+}^{trial}(\vec{r}_1, \vec{r}_a, \vec{r}_b) \middle| \hat{H}_{X^+} \middle| \Psi_{X^+}^{trial}(\vec{r}_1, \vec{r}_a, \vec{r}_b) \right\rangle, \\ E_{XX} &= \left\langle \Psi_{XX}^{trial}(\vec{r}_1, \vec{r}_2, \vec{r}_a, \vec{r}_b) \middle| \hat{H}_{XX} \middle| \Psi_{XX}^{trial}(\vec{r}_1, \vec{r}_2, \vec{r}_a, \vec{r}_b) \right\rangle. \end{aligned} \tag{9}$$

The ground state of the biexciton is a singlet state, thus the trial wave function of biexciton is not symmetric concerning electrons and holes. The trial wave function in the positronium limit $m_e^* = m_h^*$ is asymmetric, thus the energy and binding energy will be different when the electron and hole are interchanged in places.

The calculation of the quasiparticles' energies (8) allows us to obtain the binding energy for each one. The binding energies are defined below:

$$\begin{aligned} E_X^{bind} &= (E_e + E_h) - E_X, \\ E_{X^-}^{bind} &= (2E_e + E_h) - E_{X^-}, \\ E_{X^+}^{bind} &= (E_e + 2E_h) - E_{X^+}, \\ E_{XX}^{bind} &= 2E_X - E_{XX}, \end{aligned} \tag{10}$$

where E_e and E_h are the energies of the electron and hole in the SPEQD, respectively. As can be seen, the binging energy of an exciton is determined from a relative ratio of independent electron-hole pairs; correspondingly, the binding energy of a biexciton is comparable to two independent monoexcitons.

As the next step, the dependencies of the recombination energies of the discussed quasiparticles on the geometrical parameters of SPEQD have been performed. For each quasiparticle, expressions for the recombination energy are given below:

$$\begin{aligned} \omega_X^{i0} &= E_X^i, \\ \omega_{X^-}^{if} &= E_{X^-}^i - E_e^f, \\ \omega_{X^+}^{if} &= E_{X^+}^i - E_h^f, \\ \omega_{XX}^{if} &= E_{XX}^i - E_X^f. \end{aligned} \tag{11}$$

where i and f indices are the initial and final states, respectively.

The recombination energy can be defined as the difference between the initial and final states' full energies after recombination. For the case of the exciton, which consists of an electron and a hole, the recombination energy in the final state will be equal to the energy of the exciton itself in the initial state. After recombination of the electron-hole pair, the exciton remains for the biexciton, electron, and hole for the positive and negative trions, respectively.

3. Results

Let us proceed to the discussion of the results. In Figure 1, the schematic plot of the energy diagram has been shown for all excitonic complexes in comparison with the sum of energies of constituent particles, without taking into account Coulomb interactions between them, for the fixed values of the small and large semiaxes. This means that the energies are calculated as the simple amount of one particle energies with the help of Equation (6). For the exciton, it is one electron and hole; for biexciton two electrons and two holes; and one electron and two holes or two electrons and one hole, correspondingly, for positive and negative trions. Note that for all quasiparticles, the energies with the account of Coulomb

interaction lay lower than the energies without Coulomb interaction. Interestingly, the energy of the positive trion is close to the exciton energy, and the energy of the negative trion is close to the biexciton energy. The regularity, that the negative trion energy is higher than the energy of the positive trion, is because X^- consists of two electrons and one hole and X^+ consists of two holes and one electron. As the effective mass of the heavy hole is much more than the electron effective mass, the kinetic energy of the heavy hole will be much less than the electron kinetic energy.

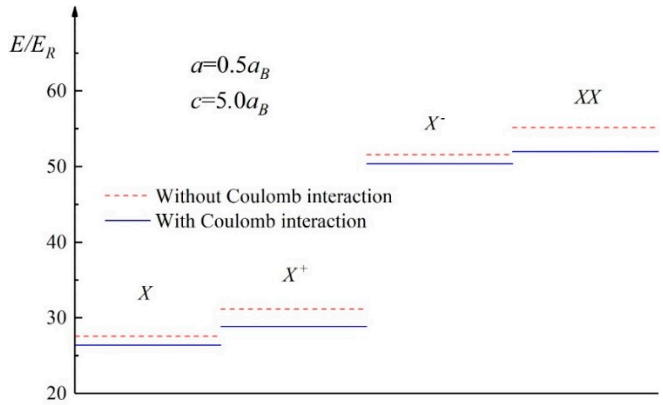

Figure 1. The schematic plot of the energy diagram for exciton (X), negative trion (X^-), positive trion (X^+), and biexciton (XX) with (blue line) and without (red dashed line) Coulomb interactions.

The comparative dependencies of the energies for all above mentioned excitonic complexes on the small semiaxis of SPEQD are shown in Figure 2. The energies for all excitonic complexes decrease with the increase of the small semiaxis. As we can see from Figure 2 for the small values of the a parameter, the energy of the biexciton is larger than the energy of the negative trion. The energy curves for these quasiparticles changed their positions with each other after a certain value of the small semiaxis. The same regularity is observed for the energy curves of the exciton and positive trion.

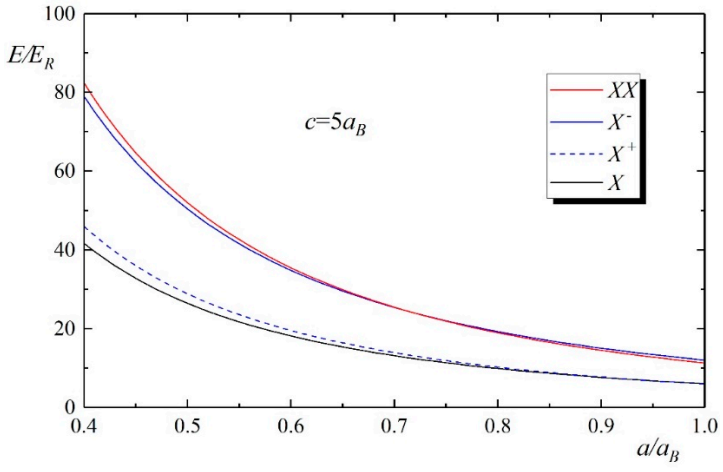

Figure 2. The comparative dependencies of the energy of the exciton (X), negative trion (X^-), positive trion (X^+), and biexciton (XX) on the small semiaxis.

In Figure 3, the dependencies of the binding energies for excitonic complexes have been presented. The binding energy for the biexciton has the biggest value; consequently, the stability of the system in SPEQD obtains a high value. The exciton and negative trion binding energies are close to each other. Therefore, the binding energy of the positive trion lays between curves for exciton and biexciton. Binding energies of the biexciton and positive trion are the maximum, while the binding energies of exciton and negative trion

monotonically increase with the increase of the small semiaxis. Although small values of the parameter, a, correspond to the large values of size quantized energy for constituent particles, nevertheless, the Coulomb interaction also increases due to the proximity of particles. That is why the curves of binding energies for all quasiparticles begin to descend with the decrease of a small semiaxis.

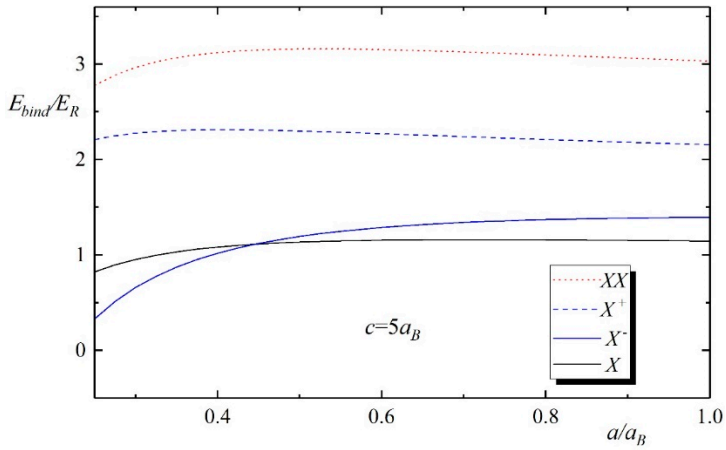

Figure 3. The comparative dependencies of the binding energy of the exciton (X), negative trion (X^-), positive trion (X^+), and biexciton (XX) on the small semiaxis.

The transitions between the ground levels for initial and final states are presented in Figure 4. The recombination energy has not been plotted for the exciton since the recombination energy of the exciton in the final state as it was described above will be equal to the energy of the exciton itself in the initial state (see Equation (10)). As can be seen from the figure, the recombination energies for the discussed quasiparticles decreases with the increase of a parameter and they are very close to each other. This proximity of curves is explained by the fact that, during the recombination process in all three complexes, one electron and one hole recombine, so the energy of the emitted photon will be approximately the same.

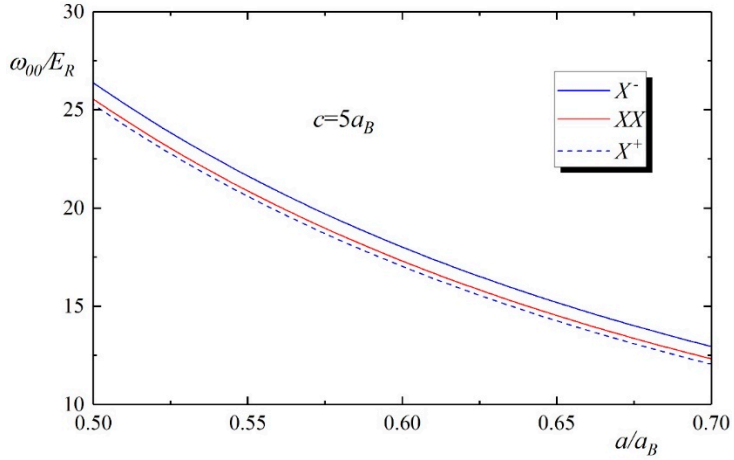

Figure 4. The comparative dependencies of the recombination energy of the negative trion (X^-), positive trion (X^+), and biexciton (XX) on the small semiaxis.

As the last step, the estimation of the exciton and biexciton lifetime in the SPEQD have been performed. The radiative lifetimes of exciton and biexciton are connected by the equation [34]:

$$\tau(XX) \simeq \frac{1}{4}\tau(X) \tag{12}$$

In its turn, the radiative lifetime of exciton and trions is determined by the equation obtained in [35,36]:

$$\tau\left(X, X^{-}, X^{+}\right) = \frac{2\pi\varepsilon_0 mc^3\hbar^2}{\sqrt{\varepsilon}e^2E^2_{(X,X^{-},X^{+})}f} \tag{13}$$

where ε_0 is dielectric constant, m is the mass of the electron, ε is the dielectric constant of the material, $E_{(X,X^{-},X^{+})}$ is the energy of excitonic complex, and f is the oscillator strength, which is defined by the formula:

$$f = \frac{E_P}{E_X}\left|\int_V \Psi_X\left(\vec{r}_e, \vec{r}_h\right)d\vec{r}\right|^2 \tag{14}$$

where E_P is the Kane energy, and for GaAs it is $E_P = 22.71eV$. The effective masses for the electron and hole are $m_e^* = 0.067m$ and $m_e^* = 0.12m_h^*$. Note that the effects of the interaction of exciton with phonons are not taken into account in Equation (13) for the exciton lifetime.

The values for the exciton, biexciton, negative, and positive trions lifetimes for different values of the geometric parameters of the SPEQD are presented in Table 1. The obtained results clearly highlight that the lifetime of all exciton complexes is directly proportional to the increase of SPEQD semiaxes. As it could have been foreseen, the probability of recombination decreases for larger localization regions.

Table 1. The lifetime of exciton complexes in strong prolate ellipsoidal quantum dot (SPEQD) for different values of semiaxes.

Large Semiaxis	Small Semiaxis	Lifetime, *ps*			
		Exciton	Positive TRION	Negative TRION	Biexciton
$c = 5a_B$	$a = 0.5a_B$	29.32	25.96	15.67	7.33
	$a = 0.7a_B$	56.57	50.08	30.24	14.14
	$a = 1a_B$	112.78	99.84	60.31	28.19
$c = 7a_B$	$a = 0.5a_B$	29.66	26.26	15.85	7.41
	$a = 0.7a_B$	57.48	50.88	30.72	14.37
	$a = 1a_B$	115.32	102.09	61.65	28.83
$c = 10a_B$	$a = 0.5a_B$	29.92	26.49	15.97	7.48
	$a = 0.7a_B$	58.17	51.54	31.16	14.54
	$a = 1a_B$	117.29	103.84	62.71	29.32

4. Conclusions

In summary, the exciton, negative and positive trions, and biexciton states in the SPEQD were calculated using the variational method. The review of the results shows that there is an inverse relationship between the binding and recombination energies for all one-dimensional quasiparticles and the a parameter. The binding energies of the biexciton and positive trion have the maximum, while the energies of the negative trion and exciton monotonically increase with the increase of the small semiaxis. It has been shown that the recombination energies of trions and biexciton are close to each other. The radiative lifetime of the one-dimensional exciton and biexciton in SPEQD made from *GaAs* is about 30 ps and 7 ps for the average values $a = 0.5a_B$ and $c = 5a_B$, respectively. Thus, manipulation of the geometrical parameters of the prolate QD brings control of the radiative lifetime of the excitonic complexes. This feature is important for the possible application of the excitonic and biexcitonic complexes as one and two-photon sources.

Funding: This research was done in the frame of the Faculty Research Funding Program implemented by the Enterprise Incubator Foundation (EIF), with the support of PMI Science.

Institutional Review Board Statement: Not applicable.

Informed Consent Statement: Not applicable.

Acknowledgments: The author would like to acknowledge his young colleagues Yuri Bleyan and Grigor Mantashian for the technical support.

Conflicts of Interest: The author declares no conflict of interest.

References

1. Hu, Y.Z.; Koch, S.W.; Lindberg, M.; Peyghambarian, N.; Pollock, E.L.; Abraham, F.F. Biexcitons in semiconductor quantum dots. *Phys. Rev. Lett.* **1990**, *64*, 1805. [CrossRef] [PubMed]
2. Patton, B.; Langbein, W.; Woggon, U. Trion, biexciton, and exciton dynamics in single self-assembled CdSe quantum dots. *Phys. Rev. B* **2003**, *68*, 125316. [CrossRef]
3. Bacher, G.; Weigand, R.; Seufert, J.; Kulakovskii, V.D.; Gippius, N.A.; Forchel, A.; Leonardi, K.; Hommel, D. Biexciton versus exciton lifetime in a single semiconductor quantum dot. *Phys. Rev. Lett.* **1999**, *83*, 4417. [CrossRef]
4. Peter, E.; Hours, J.; Senellart, P.; Vasanelli, A.; Cavanna, A.; Bloch, J.; Gérard, J.M. Phonon sidebands in exciton and biexciton emission from single GaAs quantum dots. *Phys. Rev. B* **2004**, *69*, 041307. [CrossRef]
5. Besombes, L.; Kheng, K.; Martrou, D. Exciton and biexciton fine structure in single elongated islands grown on a vicinal surface. *Phys. Rev. Lett.* **2000**, *85*, 425. [CrossRef]
6. Makarov, N.S.; Guo, S.; Isaienko, O.; Liu, W.; Robel, I.; Klimov, V.I. Spectral and dynamical properties of single excitons, biexcitons, and trions in cesium–lead-halide perovskite quantum dots. *Nano Lett.* **2016**, *16*, 2349–2362. [CrossRef]
7. Nasilowski, M.; Spinicelli, P.; Patriarche, G.; Dubertret, B. Gradient CdSe/CdS quantum dots with room temperature biexciton unity quantum yield. *Nano Lett.* **2015**, *15*, 3953–3958. [CrossRef]
8. Park, Y.S.; Bae, W.K.; Pietryga, J.M.; Klimov, V.I. Auger recombination of biexcitons and negative and positive trions in individual quantum dots. *ACS Nano* **2014**, *8*, 7288–7296. [CrossRef]
9. Ding, F.; Singh, R.; Plumhof, F.J.; Zander, T.; Křápek, V.; Chen, Y.H.; Benyoucef, M.; Zwiller, V.; Dörr, K.; Bester, G.; et al. Tuning the exciton binding energies in single self-assembled InGaAs/GaAs quantum dots by piezoelectric-induced biaxial stress. *Phys. Rev. Lett.* **2010**, *104*, 067405. [CrossRef]
10. Boero, M.; Rorison, J.M.; Duggan, G.; Inkson, J.C. A detailed theory of excitons in quantum dots. *Surf. Sci.* **1997**, *377*, 371–375. [CrossRef]
11. Li, X.; Wu, Y.; Steel, D.; Gammon, D.; Stievater, T.H.; Katzer, D.S.; Park, D.; Piermarocchi, C.; Sham, L.J. An all-optical quantum gate in a semiconductor quantum dot. *Science* **2003**, *301*, 809–811. [CrossRef] [PubMed]
12. Biolatti, E.; Iotti, R.C.; Zanardi, P.; Rossi, F. Quantum information processing with semiconductor macroatoms. *Phys. Rev. Lett.* **2000**, *85*, 5647. [CrossRef] [PubMed]
13. Holovatsky, V.A.; Holovatskyi, I.V.; Yakhnevych, M.Y. Joint effect of electric and magnetic field on electron energy spectrum in spherical nanostructure ZnS/CdSe/ZnS. *Phys. E Low Dimens. Syst. Nanostruct.* **2018**, *104*, 58–63. [CrossRef]
14. Zeng, Z.; Garoufalis, C.S.; Baskoutas, S. Combination effects of tilted electric and magnetic fields on donor binding energy in a GaAs/AlGaAs cylindrical quantum dot. *J. Phys. D Appl. Phys.* **2012**, *45*, 235102. [CrossRef]
15. Londoño, M.A.; Restrepo, R.L.; Ojeda, J.H.; Vinh Phuc, H.; Mora-Ramos, M.E.; Kasapoglu, E.S.İ.N.; Morales, A.L.; Duque, C.A. Donor impurity-related optical absorption in gaas elliptic-shaped quantum dots. *J. Nanomater.* **2017**, *2017*, 5970540. [CrossRef]
16. Baskoutas, S.; Terzis, A.F. Biexciton luminescence in InAs nanorods. *J. Appl. Phys.* **2005**, *98*, 044309. [CrossRef]
17. Xie, W. Exciton states in a disk-like quantum dot. *Phys. B Condens. Matter* **2000**, *279*, 253–256. [CrossRef]
18. Baghdasaryan, D.A.; Hayrapetyan, D.B.; Kazaryan, E.M.; Sarkisyan, H.A. Thermal and magnetic properties of electron gas in toroidal quantum dot. *Phys. E Low-Dimens. Syst. Nanostruct.* **2018**, *101*, 1–4. [CrossRef]
19. Zeng, Z.; Garoufalis, C.S.; Baskoutas, S.; Bester, G. Electronic and optical properties of ZnO quantum dots under hydrostatic pressure. *Phys. Rev. B* **2013**, *87*, 125302. [CrossRef]
20. Lampert, M.A. Mobile and immobile effective-mass-particle complexes in nonmetallic solids. *Phys. Rev. Lett.* **1958**, *1*, 450. [CrossRef]
21. Moskalenko, S.A.E.; Moskalenko, S.A.; Snoke, D.W. *Bose-Einstein Condensation of Excitons and Biexcitons: And Coherent Nonlinear Optics with Excitons*; Cambridge University Press: Cambridge, UK, 2000.
22. Hasuo, M.; Nagasawa, N.; Itoh, T.; Mysyrowicz, A. Progress in the bose-einstein condensation of biexcitons in CuCl. *Phys. Rev. Lett.* **1993**, *70*, 1303. [CrossRef] [PubMed]
23. Read, D.; Liew, T.C.H.; Rubo, Y.G.; Kavokin, A.V. Stochastic polarization formation in exciton-polariton bose-einstein condensates. *Phys. Rev. B* **2009**, *80*, 195309. [CrossRef]
24. Kavokin, A.; Malpuech, G. *Cavity Polaritons*; Elsevier: Amsterdam, The Netherlands, 2003.
25. Hayrapetyan, D.B.; Kazaryan, E.M.; Sarkisyan, H.A. Implementation of Kohn's theorem for the ellipsoidal quantum dot in the presence of external magnetic field. *Phys. E Low Dimens. Syst. Nanostruct.* **2016**, *75*, 353–357. [CrossRef]

26. Hayrapetyan, D.B.; Bleyan, Y.Y.; Baghdasaryan, D.A.; Sarkisyan, H.A.; Baskoutas, S.; Kazaryan, E.M. Biexciton, negative and positive trions in strongly oblate ellipsoidal quantum dot. *Phys. E Low Dimens. Syst. Nanostruct.* **2019**, *105*, 47–55. [CrossRef]
27. Cantele, G.; Ninno, D.; Iadonisi, G. Confined states in ellipsoidal quantum dots. *J. Phys. Condens. Matter* **2000**, *12*, 9019. [CrossRef]
28. Baghdasaryan, D.A.; Hayrapetyan, D.B.; Kazaryan, E.M. Oblate spheroidal quantum dot: Electronic states, direct interband light absorption and pressure dependence. *Eur. Phys. J. B* **2015**, *88*, 223. [CrossRef]
29. Dujardin, F.; Feddi, E.; Assaid, E. Excitonic binding energy in prolate and oblate spheroidal quantum dots. *Superlattices Microstruct.* **2018**, *114*, 296–304. [CrossRef]
30. Hayrapetyan, D.B. Direct interband light absorption in a strongly prolated ellipsoidal quantum dot. *J. Contemp. Phys.* **2007**, *42*, 292–297. [CrossRef]
31. Takagahara, T. Biexciton states in semiconductor quantum dots and their nonlinear optical properties. *Phys. Rev. B* **1989**, *39*, 10206. [CrossRef]
32. Szafran, B.; Stébé, B.; Adamowski, J.; Bednarek, S. Recombination energy for excitonic trions in quantum dots. *J. Phys. Condens. Matter* **2000**, *12*, 2453. [CrossRef]
33. Szafran, B.; Stébé, B.; Adamowski, J.; Bednarek, S. Excitonic trions in single and double quantum dots. *Phys. Rev. B* **2002**, *66*, 165331. [CrossRef]
34. Narvaez, G.A.; Bester, G.; Zunger, A. Excitons, biexcitons, and trions in self-assembled (In, Ga) As/GaAs quantum dots: Recombination energies, polarization, and radiative lifetimes versus dot height. *Phys. Rev. B* **2005**, *72*, 245318. [CrossRef]
35. Fonoberov, V.A.; Balandin, A.A. Origin of ultraviolet photoluminescence in ZnO quantum dots: Confined excitons versus surface-bound impurity exciton complexes. *Appl. Phys. Lett.* **2004**, *85*, 5971–5973. [CrossRef]
36. Sahin, M.; Koç, F. A model for the recombination and radiative lifetime of trions and biexcitons in spherically shaped semiconductor nanocrystals. *Appl. Phys. Lett.* **2013**, *102*, 183103. [CrossRef]